Chapter 5
Echocardiographic Assessment of Tricuspid Valve Disease

Thuy D. Nguyen, Jonathan M. Wong, Christiane Abouzeid, and Atif N. Qasim

Tricuspid Valve Anatomy for Echo Imaging

Knowledge of the basic tricuspid valve anatomy is essential to proper imaging of the valve to determine sites of pathology and to guide interventions. Tricuspid valve apparatus anatomy is covered in detail in Chap. 1; however, it is worthwhile to highlight several points that play a key role in imaging.

Tricuspid Leaflet Variation

The tricuspid leaflets can vary significantly in size. The septal and anterior leaflets are usually the largest in circumference compared to the posterior leaflet and are often the easiest to visualize [1]. Some individuals may have more than three leaflets, and others may functionally have two leaflets (fused or diminutive posterior leaflet). The posterior leaflet is positioned along the RV inferior wall [2].

The tricuspid leaflets are thinner than the mitral leaflets, which makes imaging more challenging [2, 3], especially when it comes to 3D imaging. Therefore,

Supplementary Information The online version contains supplementary material available at [https://doi.org/10.1007/978-3-030-92046-3_5].

T. D. Nguyen · J. M. Wong · C. Abouzeid
Department of Cardiology, University of California, San Francisco, San Francisco, CA, USA

A. N. Qasim (✉)
Division of Cardiology, Department of Medicine, University of California, San Francisco, San Francisco, CA, USA
e-mail: atif.qasim@uscf.edu

H. Mathelier et al. (eds.), *Tricuspid Valve Disease*, Contemporary Cardiology,
https://doi.org/10.1007/978-3-030-92046-3_5

Fig. 5.1 Transthoracic echocardiographic imaging of the tricuspid valve. (**a**) Right ventricular parasternal inflow. The transducer is angled inferiorly and to the right from a standard parasternal long-axis view. If the coronary sinus ostium or the muscular interventricular ventricular septum are visualized, then the leaflets imaged are the anterior (red) and septal (yellow). (**b**) Right ventricular parasternal inflow. Angling the transducer more sharply inferiorly and to the right, the posterior (blue) leaflet can be visualized instead of the septal. (**c**) Parasternal short-axis. The anterior leaflet (red) is imaged closest to the aortic valve. The posterior leaflet (blue) is most commonly the additional leaflet visualized. (**d**) Parasternal short-axis. When a single leaflet is visualized, it represents an anterior leaflet (red). (**e**, **f**) Apical four-chamber. The septal leaflet (yellow) is easily identified as the leaflet closest to the interventricular septum. However, the opposing leaflet can be either the anterior or posterior leaflet depending on angulation. Angling to include the aorta or LVOT will select for the anterior leaflet (red), whereas angling to include the coronary sinus (*) will select the posterior leaflet (blue)

knowledge of anatomy in different 2D views in both transthoracic (TTE) and transesophageal (TEE) imaging is paramount.

Standard 2D TTE Views

It is important to use multiple 2D views to identify all three leaflets and their pathology (Figs. 5.1 and 5.2) as 3D en face images may not be ideal in everyone or the view may be obscured by device leads. Only one 2D view allows one to visualize all three leaflets: the transgastric short-axis view (see Fig. 5.2f). All other 2D views allow visualization of one (typically the anterior leaflet in short-axis views) or two leaflets (either anterior-posterior, septal-anterior, or septal-posterior leaflets).

The leaflets seen in 2D views for TTE and TEE can often vary significantly in shape and position due to RV size and shape, changes in orientation of the heart within the chest, and tricuspid valve anatomical variation. However, neighboring structures can help identify each leaflet. In planes that visualize the ventricular septum, the septal leaflet should be in view; in planes that visualize the aorta, the anterior leaflet should be in view; and in planes where the coronary sinus is seen, the posterior leaflet should be seen.

Four standard TTE views are commonly utilized; these include right ventricular inflow (RVIF), parasternal short-axis (PSAX), apical four-chamber (A4C), and RV-focused (RVF) views [4]. Slight angulation changes between these views can lead to different combinations of leaflet visualization [5].

In the RVIF view, either the anterior-posterior leaflets or anterior-septal leaflets are seen. Visualization of the septum best defines the septal leaflet. If the septum is in view (incomplete rotation to remove LV and septum), then it is the septal and anterior leaflets that are seen (see Fig. 5.1a). If the LV is completely out of view, it is the posterior and anterior leaflets that are seen (see Fig. 5.1b).

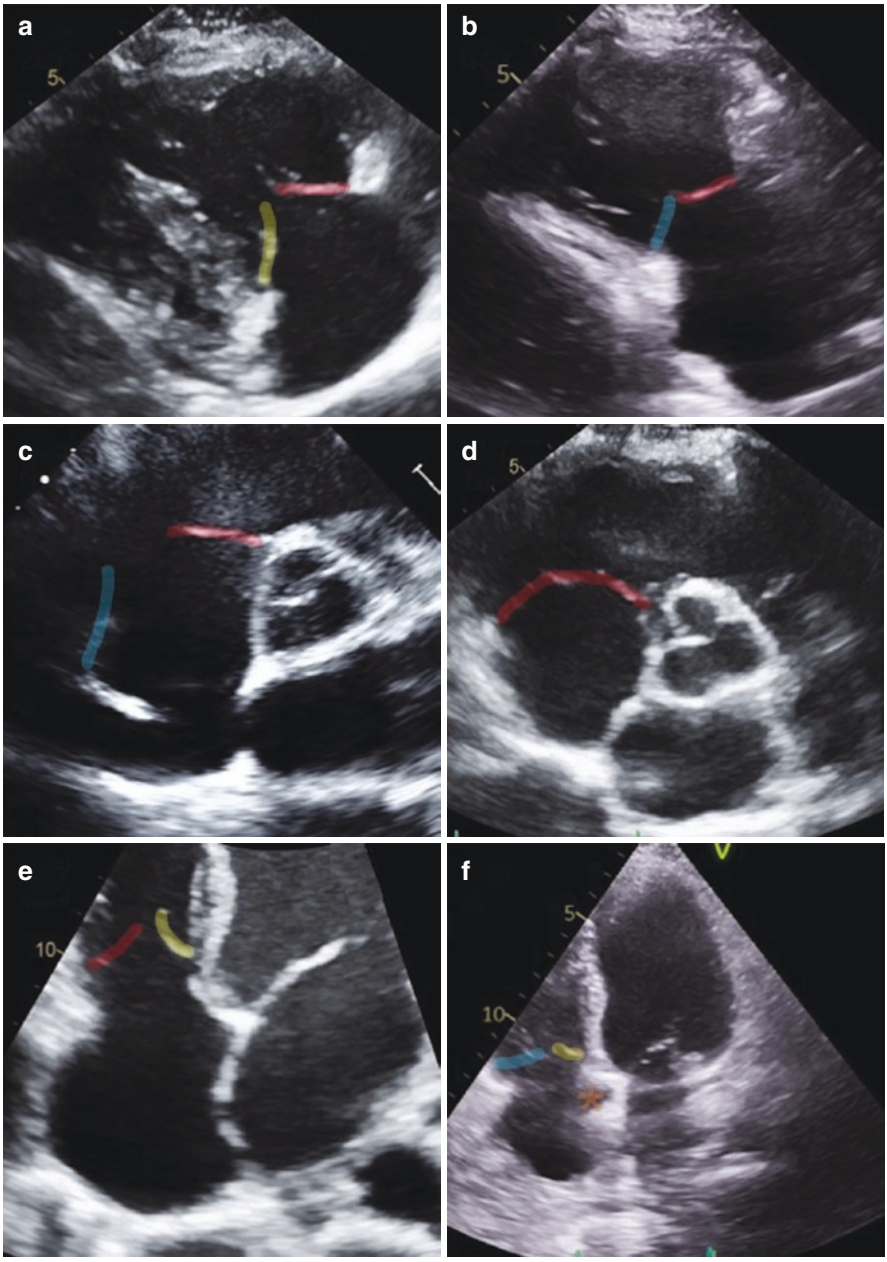

In the PSAX view, most commonly the anterior and posterior leaflets are seen, particularly when there is central coaptation (see Fig. 5.1c) [4]. If a single leaflet is seen with the aortic valve, that is the anterior leaflet, as the aorta is an anterior structure (see Fig. 5.1d) [4].

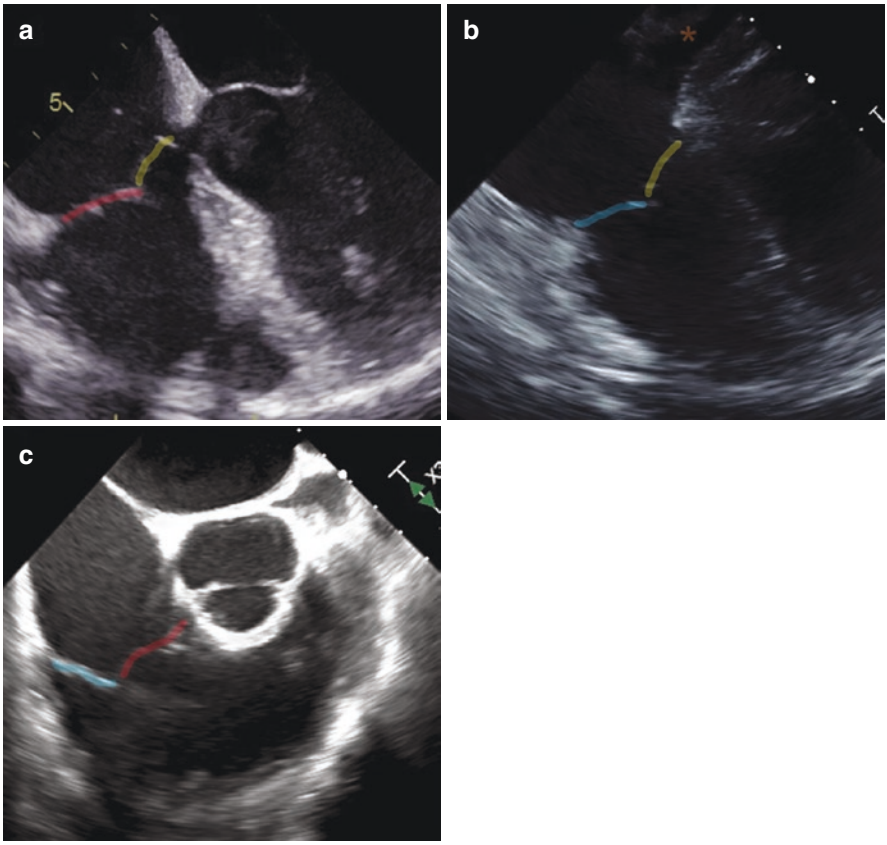

Fig. 5.2 Transesophageal echocardiographic imaging of the tricuspid valve. (**a**, **b**) Four-chamber. At 0°, either the septal-anterior leaflets or the septal-posterior leaflets are visualized. Inclusion of the LVOT or aortic valve helps identify the anterior leaflet (**a**). Inclusion of the coronary sinus (*) helps identify the posterior leaflet (**b**). (**c**) 30–70° short axis. Often it is the anterior (red) and posterior (blue) leaflets that are visualized. The septal leaflet is typically not seen in the view; however, use of multiple plane imaging can help identify this leaflet. (**d**, **e**) 30–70° short-axis orthogonal views. Orthogonal imaging through the anterior leaflet (**d**) shows the apposition of the septal (yellow) and anterior (red) leaflets. Orthogonal imaging through the posterior leaflet (**e**) identifies the apposition of the septal (yellow) and posterior (blue) leaflets. (**f**) Transgastric short axis. This 2D TEE view identifies all three leaflets en face simultaneously: anterior (red), septal (yellow), and posterior (blue). (**g**, **h**) Transgastric orthogonal views. Orthogonal imaging through the anterior leaflet (**g**) shows the apposition of the anterior (red) and posterior (blue) leaflets. Orthogonal imaging through the septal leaflet (**h**) identifies the apposition of the septal (yellow) and posterior (blue) leaflets. (**i**) Deep transgastric. In the deep transgastric view, often the septal (yellow) and anterior (red) leaflets are seen, given that this view is obtained with anteflexion when the aortic valve is in view. (**j**, **k**) Deep transgastric orthogonal views. Orthogonal imaging through the septal leaflet (**j**) shows the apposition of the septal (yellow) and posterior (blue) leaflets. Orthogonal imaging through the anterior leaflet (**k**) identifies the apposition of the anterior (red) and posterior (blue) leaflets

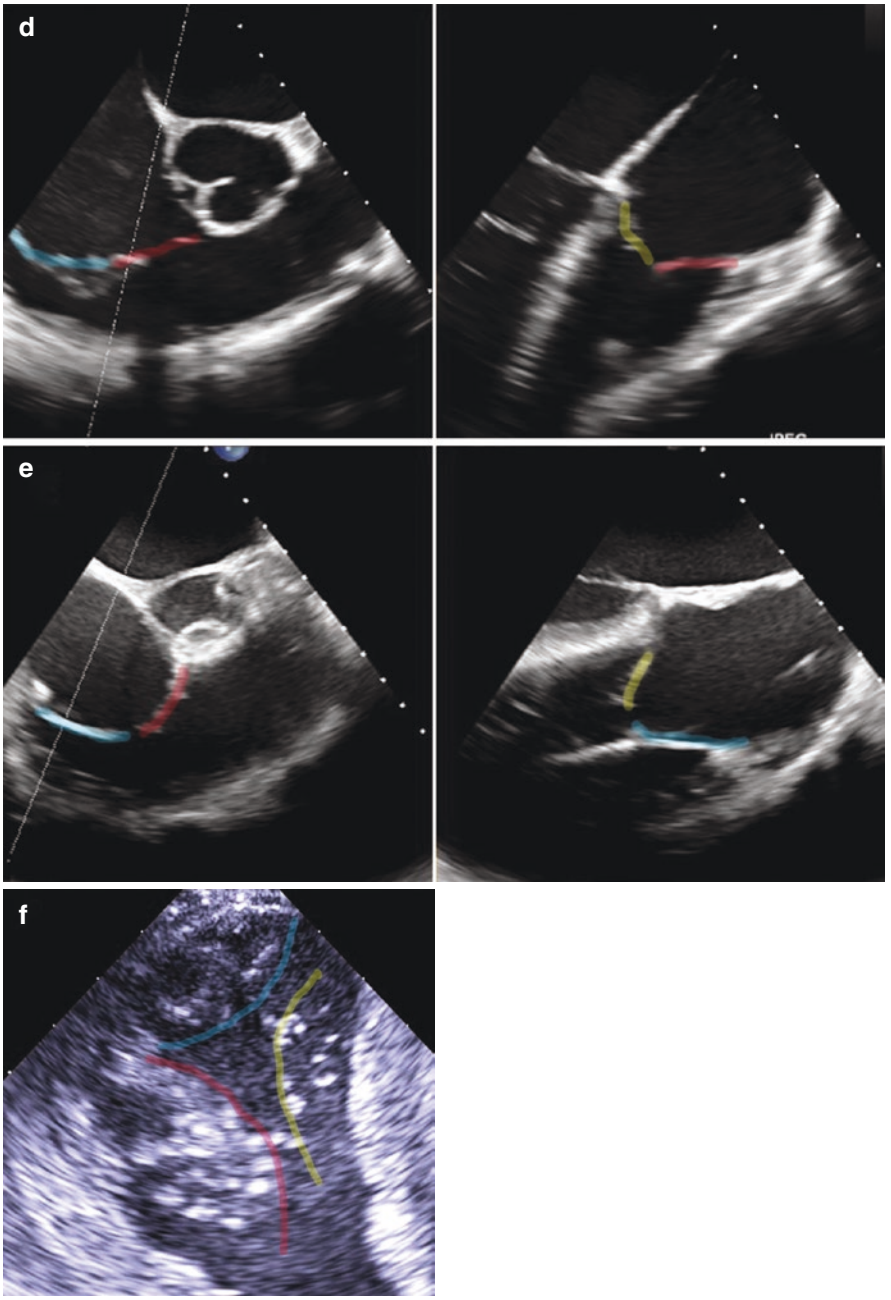

Fig. 5.2 (continued)

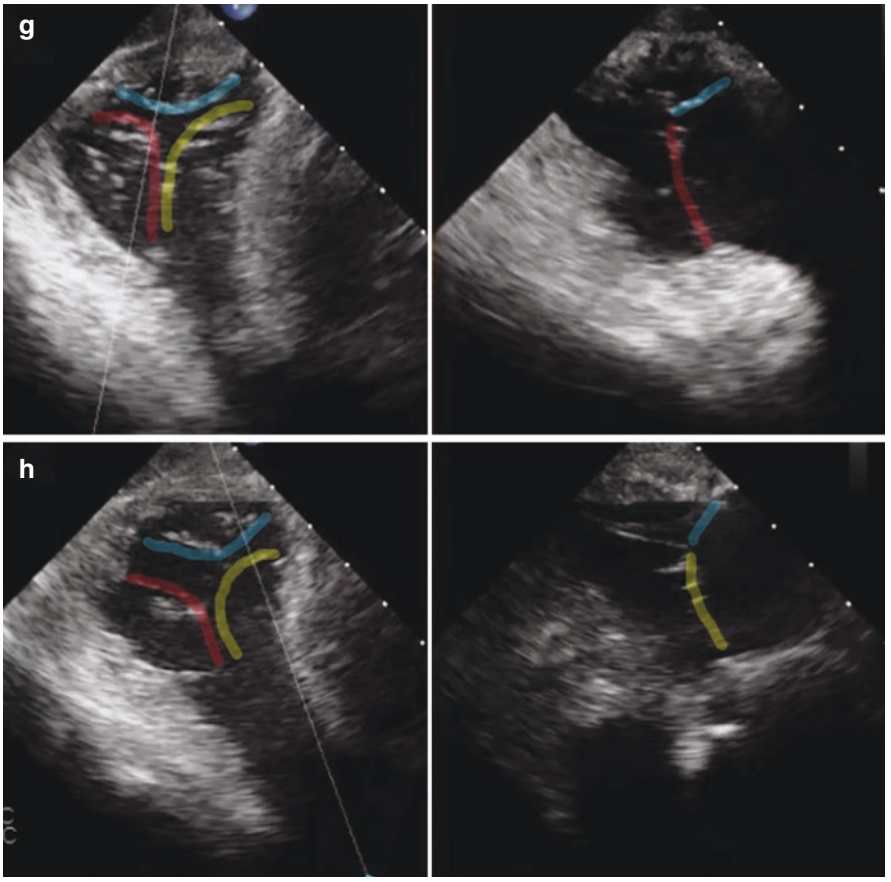

Fig. 5.2 (continued)

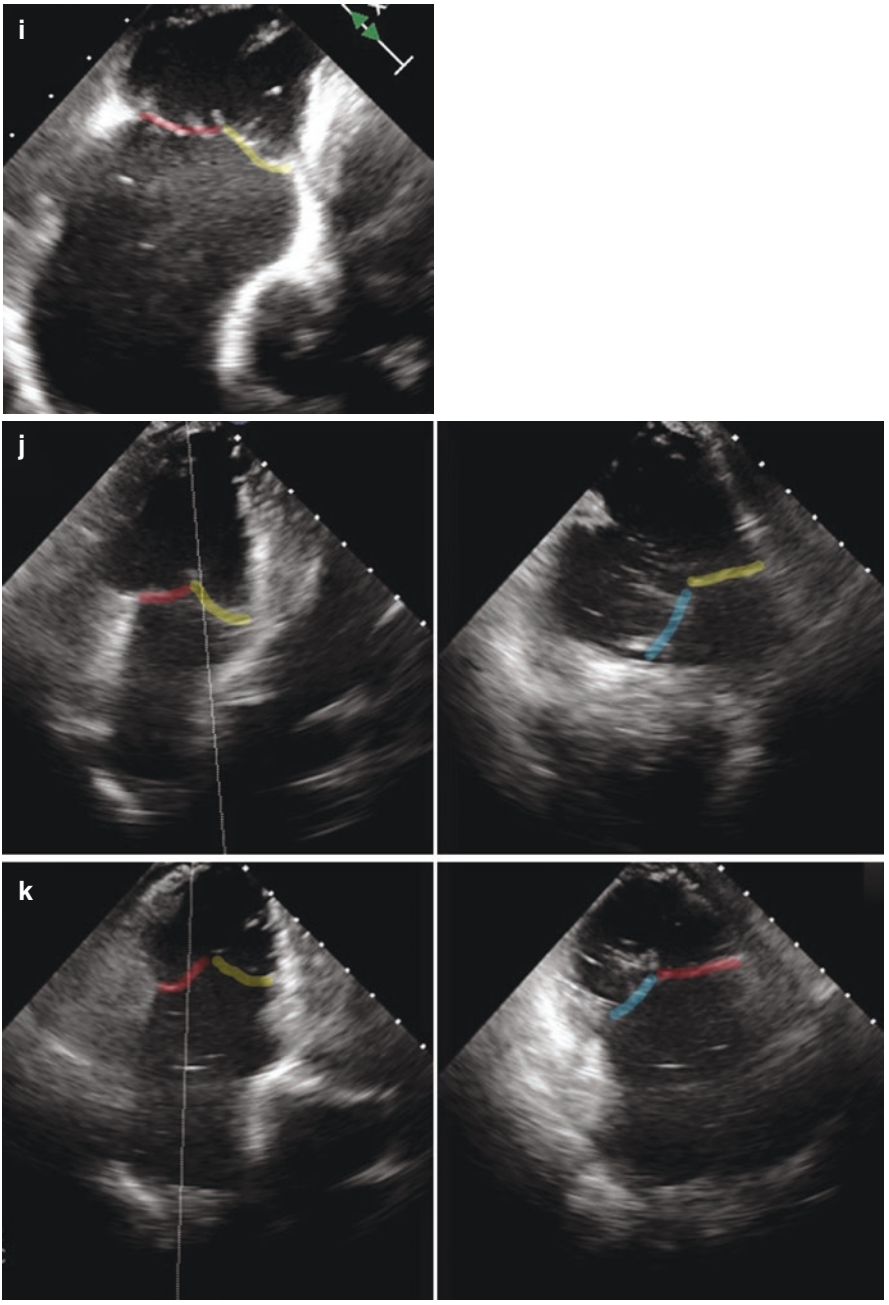

Fig. 5.2 (continued)

In the A4C window, the septal leaflet should be clearly seen—whether the other leaflet is the posterior or anterior leaflet depends on whether the probe is more anterior (visualizing part of the LV outflow tract, Fig. 5.1e) or posterior (visualizing the coronary sinus, Fig. 5.1f) [4]. The presence of the coronary sinus best defines the posterior-septal leaflets since the coronary sinus empties into the RA at the commissure of these leaflets [4]. Sweeping through the valve in real time is often helpful to discern the leaflets.

Standard 2D TEE Views

Similar principles regarding which neighboring structures are visible help identify the individual leaflets seen in the standard 2D TEE views. In the four-chamber view at 0°, either the septal-anterior leaflets or the septal-posterior leaflets are visualized. Use of anteflexion and withdrawal of the probe such that the LVOT and aortic valve starts to be seen (5-chamber view) help identify the anterior leaflet (Fig. 5.2a). Insertion and retroflexion of the probe help identify the posterior leaflet, especially when the coronary sinus comes into view (Fig. 5.2b).

In the short-axis view (30–70°) just as in the parasternal short-axis view for TTE, often it is the anterior and posterior leaflets that are visualized (Fig. 5.2c). The septal leaflet is typically not seen in the view; however, use of multiple plane imaging can help identify this leaflet as well as associated pathology (lack of coaptation, tethering). Orthogonal imaging through the anterior leaflet (closest to the aorta) shows the apposition of the septal and anterior leaflets, and orthogonal imaging through the posterior leaflet identifies the apposition of the septal and posterior leaflets (Fig. 5.2d, e). These views can then be individually assessed in corresponding planes (110–150°) if needed.

The transgastric views are often the most helpful to identify leaflets in patients with devices or leads since shadowing from these structures is less of an issue. The short axis here is the only 2D TEE view that clearly identifies all three leaflets en face simultaneously (Fig. 5.2f). From here, additional orthogonal plane imaging can be used to visualize either anterior-posterior (Fig. 5.2g) or septal-posterior leaflets (Fig. 5.2h). In the deep transgastric view, which is similar to a TTE four-chamber view, often the septal-anterior leaflets are seen, given that this view is obtained with anteflexion and often the aortic valve is in view (Fig. 5.2i). Orthogonal planes show the septal and posterior leaflets and the anterior and septal leaflets (Fig. 5.2j, k).

3D Views

It is important to decide on a convention when imaging the tricuspid valve en face in 3D. This is critical when working with a team to plan interventional procedures. Some advocate for displaying the interatrial septum, and thus septal leaflet, inferiorly in the far field at 6 o'clock [5]; however, others display this leaflet at 9 o'clock

similar to a surgeon's view, in keeping with the convention for mitral valve views. The general rule of thumb is to start with the best 2D image (whether at 0°, short axis, or possibly even deep transgastric) in the mid-esophageal views and then to acquire the 3D images. Including a neighboring structure, such as the aortic valve as a landmark, helps one to better rotate and orient the image into an ideal view. Figure 5.3 shows several examples of 3D en face views that help identify some of

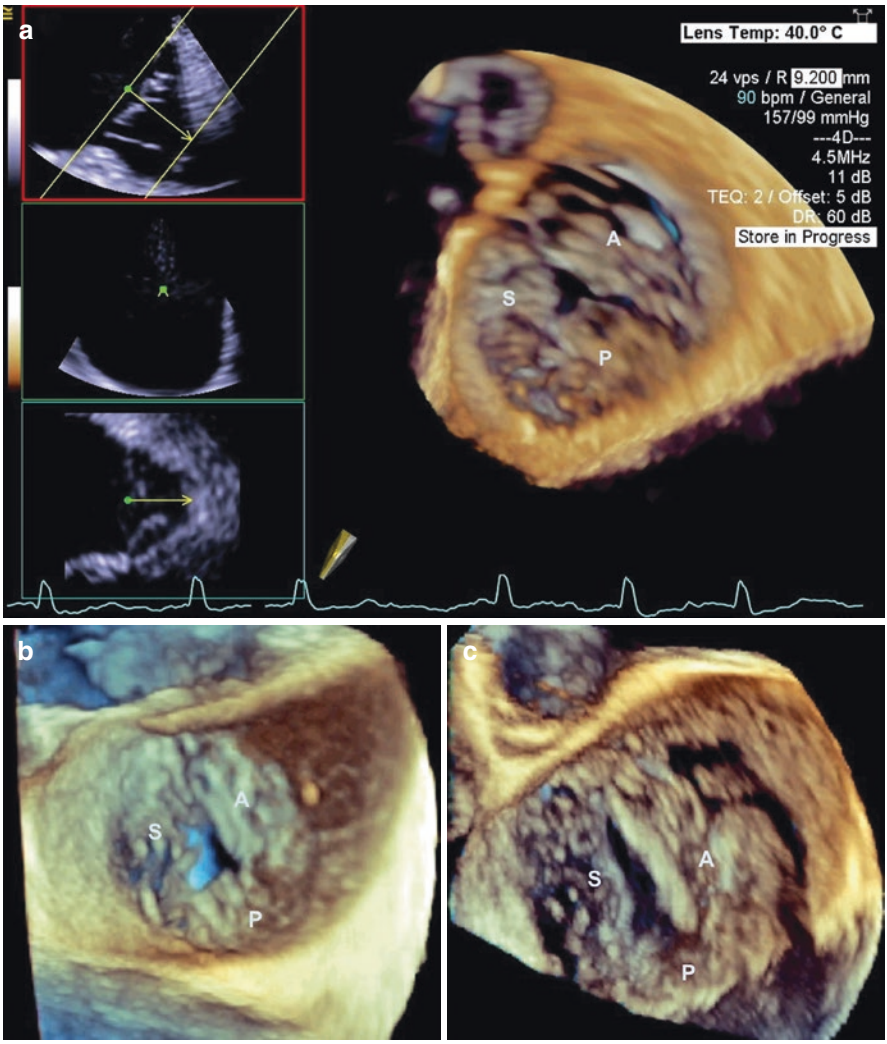

Fig. 5.3 3D en face views of the tricuspid valve. (**a**) An example where all three tricuspid leaflets are of similar size and their commissures are easy to identify. (**b**) Partially fused anterior and posterior leaflets. (**c**) Diminutive posterior leaflet with large anterior and septal leaflets. (**d**) Reconstructed en face view from 3D data set showing orthogonal 2D views that bisect the leaflets at their point of coaptation

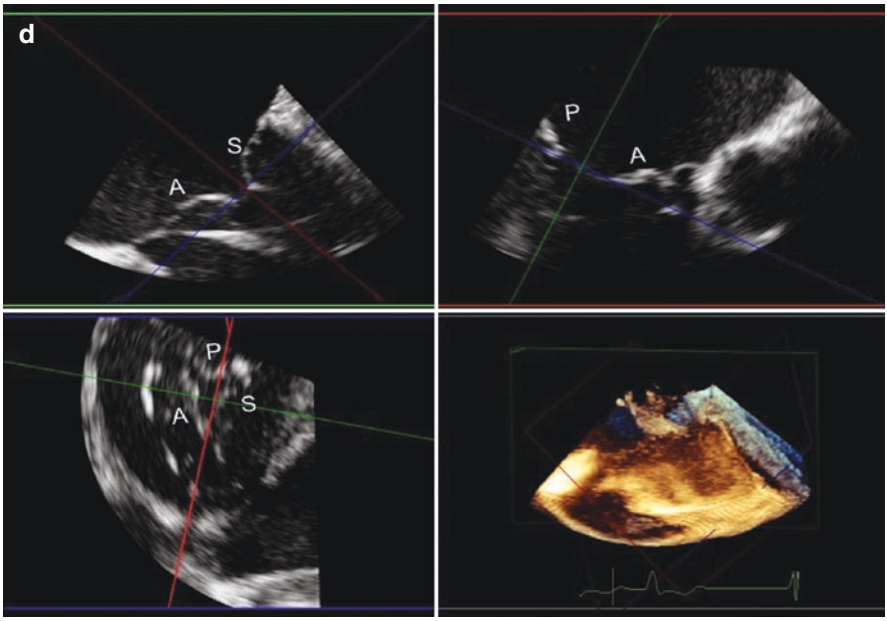

Fig. 5.3 (continued)

the variations in leaflet anatomy mentioned above. Figure 5.3d shows reconstruction of orthogonal planes from a 3D data set to help create an en face view similar to the transgastric image. This reconstruction can be useful for making annular and valvular measurements.

Annulus Sizing

Similar to the mitral annulus, the tricuspid annulus (TA) is nonplanar and has a dynamic shape during the cardiac cycle [1]. An understanding of shape changes helps make the appropriate measurements needed to identify pathological enlargement. In RV diastole, the TA takes on an elliptical, saddle shape with peaks at the anteroseptal and posterolateral portions and conversely, lower points at its anterolateral and posteroseptal portions [3]. In normal hearts, the TA morphology flattens and becomes more circular during RV systole [1, 6].

The diameter and the circumference of the TA are also dynamic so that measurements vary within the cardiac cycle [2]. Change in size largely occurs in the septolateral direction since the septal leaflet is relatively fixed and dilation occurs with gaps between the septal-anterior or septal-posterior leaflets. The TA appears largest in end RV diastole and smallest in RV systole [1, 2, 7]. Multiple publications note that normal TA size is affected by gender and body surface area (BSA) [1, 2, 7].

These alterations have led to some disagreement across publications on normal size, as well as when and in which plane to make optimal measurements [7]. The European guidelines currently describe a normal TA diameter in an adult as 28 ± 5 mm at *end diastole* in the A4C echocardiographic view [1, 8]. The European and American guidelines are in agreement and define a dilated TA diameter in an adult at >40 mm (>21 mm/m^2) in diastole on the A4C echocardiographic view [1, 9]. However, these guidelines are not based on surgical outcomes, and studies have shown that 2D echocardiographic measurements underestimate TA size when compared to 3D echocardiography, MRI, or multidetector CT [2, 3, 7].

It is important with annular size measurements to decide whether the mechanism of tricuspid regurgitation is due to annular dilation, leaflet tethering, or both. Leaflet tethering often occurs in tandem with RV dilation in the mid and distal segments; this can be observed in processes such as pulmonary hypertension. Annular anatomy may be preserved, but leaflet tenting may exist. In primary annular pathologies, which may be seen in patients with enlarged atria, atrial fibrillation, or other causes of functional TR such as primary right ventricular cardiomyopathies, the base may dilate significantly, and the leaflets become flat and fail to coapt. The coaptation gap can often be much greater than that seen with the mitral valve; this results in torrential tricuspid regurgitation and is important to characterize to plan interventional procedures.

Assessing Mechanism of Tricuspid Regurgitation or Stenosis and Severity

The etiology of tricuspid valve pathology is diverse but predominantly results in regurgitation rather than stenosis. In a 25-year surgical pathology series from the Mayo clinic, 74% of tricuspid valves were purely regurgitant and 2% were purely stenotic [10]. The severity of regurgitation and stenosis dictates the presence and extent of clinical manifestations and predicts cardiovascular outcomes [11]. Hemodynamically significant tricuspid regurgitation or stenosis leads to right heart failure, which may manifest as peripheral edema, hepatomegaly with hepatic congestion, and distended neck veins. Echocardiography is critical to identify etiology and then appropriately classify the severity of tricuspid valve disease.

Tricuspid Regurgitation

In 80–90% of normal individuals, tricuspid regurgitation is identified on echocardiography [12]. However, <1% of these individuals have moderate or greater tricuspid regurgitation. Tricuspid regurgitation can be classified into primary and secondary etiologies (Table 5.1). In a series of patients with severe tricuspid regurgitation by echocardiography, only 9.5% of patients were found to have organic

Table 5.1 Causes of tricuspid regurgitation

Primary (20%)	Secondary (80%)
Myxomatous	Left heart disease (valve disease, LV dysfunction)
Rheumatic	Any cause of pulmonary hypertension
Endocarditis	Any cause of RV dysfunction
Carcinoid syndrome	
Drug-induced (anorectic drugs, fenfluramine)	*Idiopathic* (associated with atrial fibrillation)
Traumatic (blunt chest injury, laceration)	
Iatrogenic (device lead, RV biopsy)	
Congenital (Ebstein's anomaly)	

Adapted from Ref. [6]

tricuspid disease [13]. Approximately 75–80% of patients with significant tricuspid regurgitation were found to have a functional etiology for their disease [14].

Native Primary Tricuspid Regurgitation

Characteristic echocardiographic features distinguish the etiology of primary tricuspid regurgitation. The prevalence of concomitant myxomatous tricuspid and mitral disease is uncertain. In a study of patients with mitral valve prolapse, tricuspid prolapse was also present in 10–20% of patients [15]. Isolated myxomatous degeneration of the tricuspid valve is much less common than myxomatous degeneration of the mitral valve, with autopsy studies suggesting a prevalence of 0.3–3% [16]. Relative to left-sided valves, surgical intervention of primary myxomatous tricuspid disease is uncommon, seen in 4% of patients in a series from Beijing [14]. The appearance of myxomatous tricuspid valves on echocardiography is similar to features noted in mitral disease, which can include thickened and billowed leaflets with prolapse and flail segments (Fig. 5.4a).

Fig. 5.4 (**a**) Tricuspid valve prolapse. Left: Right ventricular parasternal inflow view showing prolapse and billowing (arrow) of the septal leaflet (Video 5.1a). The coronary sinus is also seen (*). Right: Zoomed right ventricular parasternal inflow view with color Doppler showing eccentric jet away from the prolapsed leaflet (see Video 5.1a). (**b**) Rheumatic heart disease. Apical four-chamber view showing thickening and restriction of the tricuspid leaflets as well as annular dilation and an enlarged large RA (Video 5.1b). There is also significant RV dilation and tethering of the tricuspid leaflets in the setting of pulmonary hypertension leading to a large coaptation gap between tricuspid leaflets. This patient also has severe mitral and aortic stenosis in the setting of rheumatic heart disease. (**c**) Carcinoid. Upper left: Right ventricular parasternal inflow view showing reduced mobility of the tricuspid valve in a patient with carcinoid tricuspid valve disease (Video 5.1c). Upper Right: Diastolic color flow acceleration through the tricuspid valve (see Video 5.1c). Bottom: Continuous wave Doppler through the tricuspid valve showing tricuspid regurgitation with pulmonary hypertension and tricuspid stenosis. (**d**) Ebstein's anomaly. Apical four-chamber view showing severe apical displacement of the septal leaflet of the tricuspid valve (arrow) and right-sided chamber dilation (Video 5.1d)

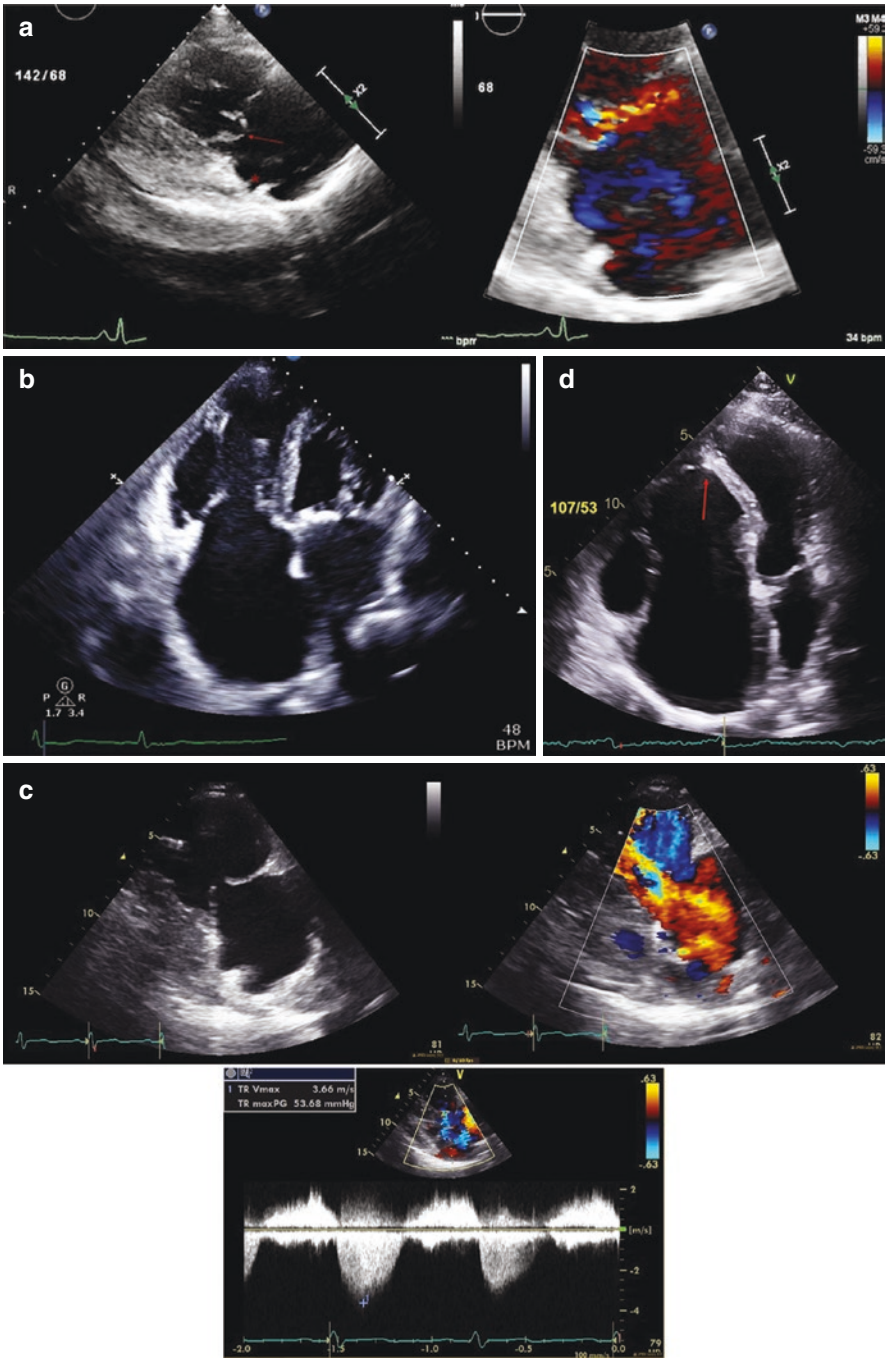
a
142/68
68
34 bpm
b
48
BPM
d
107/53
c
1 TR Vmax 3.66 m/s
TR maxPG 53.68 mmHg

Rheumatic disease is the most common cause of primary tricuspid regurgitation in developing countries. Rheumatic tricuspid disease can also manifest long after mitral valve replacement [17]. Surgical intervention for isolated tricuspid disease is rare. Of 328 consecutive patients who underwent tricuspid surgery for rheumatic disease in a Spanish series, only 4% had isolated tricuspid surgery [18]. The appearance of rheumatic disease in the tricuspid position on echocardiography is similar to its appearance on the mitral valve, with restricted leaflet motion and leaflet shortening and thickening. Often, many patients with rheumatic mitral valve disease will have atrial fibrillation with large RA and annular dilation as well as significant right ventricular dilation and dysfunction with pulmonary hypertension. This causes tricuspid regurgitation through multiple mechanisms as shown in Fig. 5.4b.

Carcinoid tumors, which constitute a rare form of malignancy that originates from enterochromaffin cells in the gastrointestinal tract, may secrete significant vasoactive substances such as serotonin. This process can lead to the deposition of fibrous tissue, or carcinoid plaque, onto the tricuspid valve [19]. The valve leaflets typically remain intact while the ventricular aspect of the tricuspid valve is often affected. On echocardiography, the tricuspid leaflets are thickened, and mobility is significantly reduced (Fig. 5.4c); usually, this causes combined regurgitation and stenosis [20].

The cause of primary tricuspid regurgitation in young adults is often congenital, with Ebstein's anomaly as the most common. Ebstein's anomaly, however, is rare, occurring in <1 per 200,000 live births [21]. It is characterized by adherence of the septal and posterior leaflets to the myocardium due to failure of delamination, as well as apical displacement of the functional annulus, dilation of the "atrialized" right ventricle with associated "true" annular dilation, and tethering and abnormalities of the anterior leaflet. An atrial communication is also almost always present; this occurs in up to 90% of patients [22]. The diagnosis is supported by >8 mm/m^2 apical displacement of the tricuspid valve as compared to the mitral valve [23]. Other common echocardiographic findings include exaggerated motion of the anterior leaflet, abnormal chordal attachments to the septal leaflet, right ventricular outflow tract dilation, significant tricuspid regurgitation, and interatrial shunt with right-to-left shunting due to increased right atrial pressures (Fig. 5.4d). Ebstein's anomaly may vary in the severity of anatomic derangement, correlating with the amount of leaflet displacement and tethering, as well as right ventricular dilation and dysfunction [21].

Primary tricuspid regurgitation can also be iatrogenic; this can occur following procedures that require traversing the tricuspid valve, such as right ventricular biopsy and cardiac electronic device (CED) implantation. The incidence of worsening tricuspid regurgitation after CED implantation varies; it can occur as frequently as in 45% of patients [24]. CED leads traversing the tricuspid valve can lead to leaflet impingement, adherence, perforation, laceration, and subvalvular interference [25], of which echocardiography may assist with diagnosis (Fig. 5.5). A tricuspid regurgitation jet that originates more apically than the coaptation point suggests lead interference. 3D echocardiography may improve the ability to determine lead trajectory [26, 27]. Leads located in the valve commissures or center of the valve

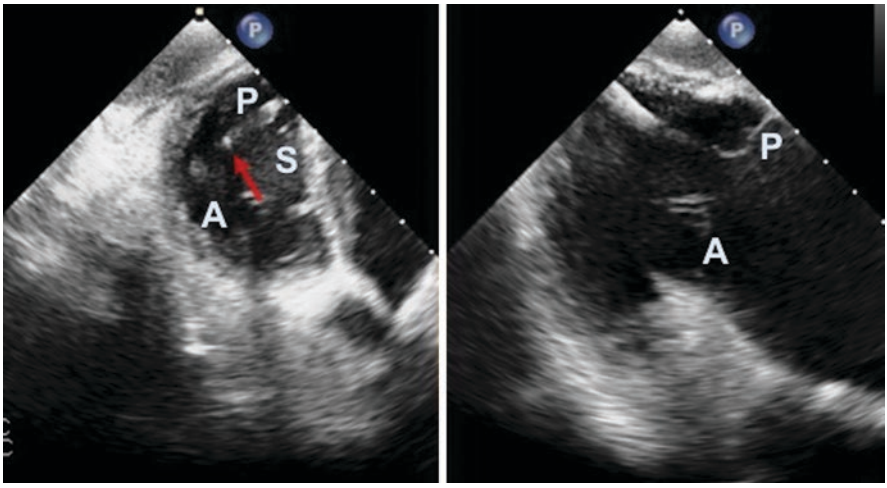

Fig. 5.5 Tricuspid regurgitation from cardiac electronic device lead impingement. Orthogonal transgastric views of the tricuspid valve (Video 5.2). A cardiac electronic device lead is seen tethering the posterior leaflet (arrow) and contributing to severe tricuspid regurgitation

were less associated with significant tricuspid regurgitation compared to leads adherent to the leaflets [27]. CEDs may also lead to right ventricular remodeling, another potential mechanism of CED-associated tricuspid regurgitation [28].

Native Secondary Tricuspid Regurgitation

Secondary or "functional" tricuspid regurgitation is more common than primary tricuspid regurgitation. Secondary tricuspid regurgitation can be further defined by etiology: left heart disease, pulmonary hypertension, idiopathic annular dilation in the setting of atrial myopathies and atrial fibrillation, and primary right ventricular dysfunction (see Table 5.1). In the setting of pulmonary hypertension, there is right ventricular remodeling and lengthening, often with dilation at the mid-wall and apical displacement of the tricuspid subvalvular apparatus leading to leaflet tethering and a coaptation gap (Fig. 5.6a). With primary RV cardiomyopathies as can be seen with ARVC, there can be tricuspid annular dilation, which causes the saddle-shaped annulus to become flat and circular, as there is progressive dilation in the direction of the free wall [29] (Fig. 5.6b). The degree of functional tricuspid regurgitation is independently prognostic in left heart disease [30], pulmonary hypertension [31], and right ventricular dysfunction [11].

Sometimes referred to as "idiopathic" or "isolated," tricuspid regurgitation associated with atrial fibrillation is another common functional cause [13]. In this condition, the predominant mechanism is excessive annular enlargement in the direction of the free wall (Fig. 5.6c), with isolated basal right ventricular enlargement and

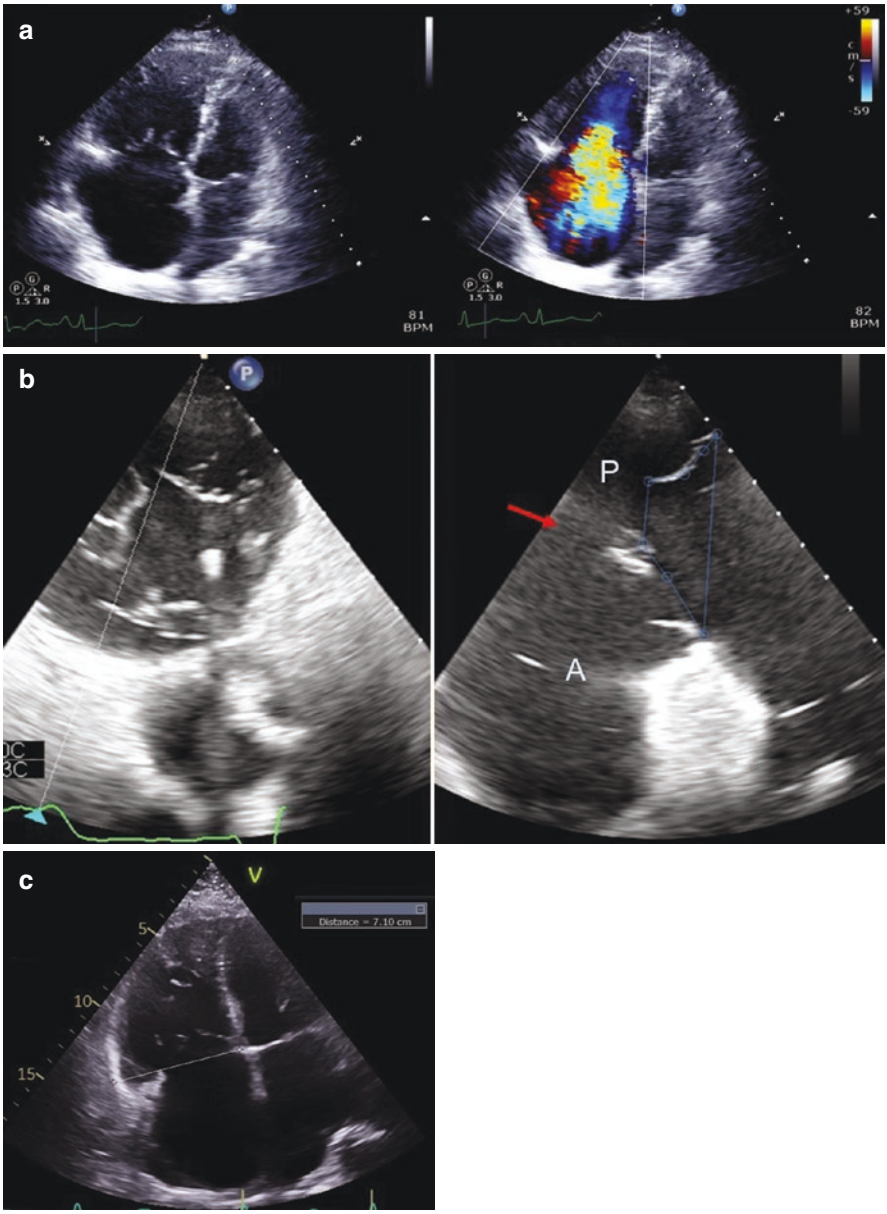

Fig. 5.6 Secondary tricuspid regurgitation examples. (**a**) Tricuspid regurgitation due to pulmonary hypertension. Note the tethering of the tricuspid leaflets and lack of significant annular dilation leading to severe tricuspid regurgitation, with the origin of the color jet well below the annular plane (Video 5.3a). (**b**) Tricuspid regurgitation due to arrhythmogenic right ventricular cardiomyopathy. Left: Transgastric view of the tricuspid valve during early systole (Video 5.3b). Right: Orthogonal view across the posterior and anterior leaflets (see Video 5.3b). This patient has severe RV dysfunction and torrential tricuspid regurgitation, with a significant tenting area (blue outline) and coaptation gap (red arrow). (**c**) Idiopathic tricuspid regurgitation. Right ventricular focused apical four-chamber view in early systole showing severe RV enlargement, tricuspid annular dilation, and tricuspid leaflet malcoaptation (Video 5.3c). This patient has idiopathic tricuspid regurgitation from atrial fibrillation

right atrial enlargement [29]. The tricuspid leaflet tethering area is typically negligible, in contrast to tricuspid regurgitation due to right ventricular dysfunction and lengthening. This etiology of tricuspid regurgitation is associated with advanced age, female gender, small body surface area, and hypertension [32]. Severe tricuspid regurgitation from idiopathic tricuspid regurgitation is also independently associated with increased morbidity and mortality [33, 34]. In secondary tricuspid regurgitation, a comprehensive echocardiographic evaluation involves assessing left heart chambers and valves, pulmonary vasculature, right ventricular remodeling and function, tricuspid leaflet tethering, tricuspid annulus assessment, and tricuspid regurgitation severity [35].

Echocardiographic Assessment of Tricuspid Regurgitation Severity

Echocardiography remains the most common and comprehensive method to assess the severity of tricuspid regurgitation. Cardiac magnetic resonance and computer tomography angiography are other noninvasive modalities that can be used to quantitate and assess tricuspid valve regurgitation, each with its own advantages and disadvantages. To characterize native tricuspid regurgitation severity, the American Society of Echocardiography guidelines [36] suggest a comprehensive assessment using structural, qualitative, semiquantitative, and quantitative parameters (Table 5.2).

Color Doppler jet area is affected by many parameters, including power, gain, tissue priority setting, aliasing velocity, and jet eccentricity [37]. Relative to a mitral regurgitant jet, the color jet area tends to be smaller in tricuspid regurgitation for a given EROA due to lower velocities and conservation of momentum [38]. The vena contracta, or a measurement of the color jet at its narrowest point, can be performed in 2D (width) or 3D (area) echocardiography. 3D analysis reveals that the vena contracta is often ellipsoid or crescent shape [39]; therefore, 2D methods may vary based on the imaging window. Continuous-wave velocity profile, another qualitative assessment using Doppler, is weak and incomplete in trivial or mild tricuspid regurgitation. The spectral envelope becomes dense, complete, and triangular with severe tricuspid regurgitation, as right atrial pressure rises early in systole.

Systolic flow reversal in the hepatic vein is a common sign of severe tricuspid regurgitation but is not specific and can also occur in ventricular or junctional rhythm with retrograde P-waves [37]. There is no regurgitation volume cutoff to produce systolic reversal of the hepatic vein. Small right atrial volume, elevated systemic venous pressure, and reduced right ventricular function require a lesser degree of tricuspid regurgitation to produce a systolic reversal of the hepatic vein [37].

Quantitative assessment can be performed using proximal convergence and volumetric quantification analysis [36]. The PISA method takes advantage of the aliasing velocity and assumes that blood approaches the regurgitant valve at hemispheric isovelocity shells, which allows for an estimate of flow. Using the conservation of mass, EROA can be calculated by dividing the flow into the maximal velocity from

Table 5.2 Grading the severity of tricuspid regurgitation by echocardiography

Structural	Mild	Moderate	Severe
TV morphology	**Normal or mildly abnormal leaflets**	Moderately abnormal leaflets	**Severe valve lesions** (e.g., flail leaflet, severe retraction, large perforation)
RV and RA size	Usually normal	Normal or mild dilation	Usually dilated[a]
IVC diameter	Normal <2 cm	Normal or mildly dilated (2.1–2.5 cm)	Dilated >2.5 cm
Qualitative Doppler			
Color flow jet area[b]	**Small, narrow, central**	Moderate central	**Large central jet** or eccentric wall-impinging jet of variable size
Flow convergence zone	**Not visible, transient or small**	Intermediate in size and duration	**Large throughout systole**
CWD jet	**Faint/partial/** parabolic	Dense, parabolic or triangular	Dense, often triangular
Semiquantitative			
Color flow jet area (cm^2)[b]	Not defined	Not defined	**>10**
VCW (cm)	<0.3	0.3–0.69	**≥0.7**
PISA radius (cm)[c]	≤0.5	0.6–0.9	**>0.9**
Hepatic vein flow[d]	Systolic dominance	Systolic blunting	**Systolic flow reversal**
Tricuspid inflow[d]	**A-wave dominant**	Variable	E-wave >1.0 m/s
Quantitative			
EROA (cm^2)	<0.20	0.20–0.39[e]	**≥0.40**
RVol (2D PISA) (mL)	<30	30–44[e]	≥0.45

Adapted from Ref. [29]
Bolded signs are considered specific for their TR grade
CWD continuous-wave Doppler, *EROA* effective regurgitant orifice area, *IVC* inferior vena cava, *PISA* proximal isovelocity surface area, *RA* right atrium, *RV* right ventricle, *RVol* regurgitant volume, *VCW* vena contracta width
[a]RV and RA size can be within the "normal" range in patients with acute severe TR
[b]With Nyquist limit >50–70 cm/s
[c]With baseline Nyquist limit shift of 28 cm/s
[d]Signs are nonspecific and are influenced by many other factors (RV diastolic function, atrial fibrillation, RA pressure)
[e]There are too little data to support further separation of these values

the continuous wave Doppler. Geometric and temporal assumptions limit the accuracy of the PISA method, as EROA is often underestimated. Volumetric assessment compares the stroke volume through the regurgitant valve with a reference stroke volume, often the LVOT [37]. The tricuspid valve annulus can be measured using 2D biplane or 3D. The EROA can also be estimated directly using 3D color vena contracta. The echocardiographic features of severe tricuspid regurgitation are

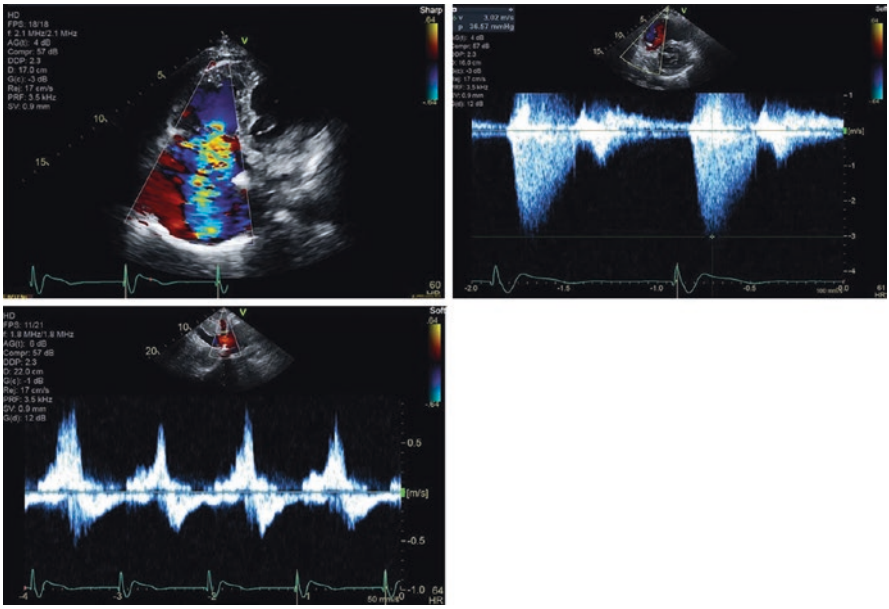

Fig. 5.7 Features of severe TR. Upper Left: Color Doppler jet area >10 cm^2 (Video 5.4). Upper Right: Triangular continuous-wave tricuspid regurgitation signal. Bottom: Systolic reversal of the hepatic vein flow in the subcostal window

Table 5.3 Proposed new grading system for tricuspid regurgitation

Parameters	Mild	Moderate	Severe	Massive	Torrential
VC width[a]	<3 mm	3–6.9 mm	7–13 mm	14–20 mm	≥21 mm
EROA (PISA)	<20 mm^2	20–39 mm^2	40–59 mm^2	60–79 mm^2	≥80 mm^2
3D VC area			75–94 mm^2	95–114 mm^2	≥115 mm^2

Adapted from Ref. [29]
EROA effective regurgitant orifice area, *PISA* proximal isovelocity surface area, *VC* vena contracta
[a]VC width calculated by the average of two orthogonal views

shown in Fig. 5.7. Due to the frequent late presentation of tricuspid regurgitation, a new proposed grading system for tricuspid regurgitation has been proposed (Table 5.3) but has not been validated [40]. Whereas the EROA can exceed 3–4 times the severe cutoff in tricuspid regurgitation with obvious non-coaptation, this is not compatible with life in mitral regurgitation.

Native Tricuspid Stenosis

Tricuspid valve obstruction is a rare entity. In adults, it is most commonly caused by rheumatic disease but is also caused by congenital abnormalities, metabolic disorders (carcinoid, Fabry's disease, Whipple's disease), and endocarditis [41]. Tricuspid

stenosis is rarely isolated when it is due to rheumatic disease. Echocardiographic findings that are consistent with severe tricuspid stenosis include mean pressure gradient ≥5 mmHg, inflow time-velocity integral >60 cm, pressure half time ≥190 ms, and valve area ≤1 cm^2 [42].

Prosthetic Tricuspid Disease

Bioprosthetic valves are more common than mechanical valves in the tricuspid position due to the risk of valve thrombosis. The echocardiographic assessment of prosthetic tricuspid valve is similar to that of native tricuspid disease. The complications of prosthetic tricuspid disease are similar to other prosthetic valve diseases, which include obstruction from pannus, thickening, or calcification, as well as paravalvular leak, leaflet tear, valve dehiscence, thrombus, or vegetation.

Given that prosthetic velocities vary with respiration, an average of five cardiac cycles should be used regardless of underlying rhythm [43]. Although limited data exist, prosthetic EOA can be calculated by measuring the LVOT stroke volume by the prosthesis VTI; however, the presence of significant tricuspid regurgitation will not be accurate. There is a suggestion of prosthetic tricuspid stenosis if peak velocity reaches >1.7 m/s and the mean gradient is ≥6 mmHg, with a pressure half time of ≥230 ms (Fig. 5.8). Prosthetic tricuspid regurgitation is suggested if jet area >10 cm^2, vena contracta width >0.7 cm, and systolic reversal of the hepatic vein is present, and if the jet contour and density are early peaking and dense. Conversely, bioprosthetic tricuspid parameters were obtained shortly after surgery in a Mayo Clinic series, with "normal values" that include pressure half time <200 ms, mean gradient <9 mmHg, E velocity <2.1 m/s, tricuspid VTI <66 cm, and VTI (TV)/VTI (LVOT) <3.3 [44]. Similarly, normal mechanical tricuspid prosthetic echocardiographic parameters shortly after surgery were pressure half time <130 ms, peak E velocity <1.9 m/s, and mean gradient <6 mmHg [45].

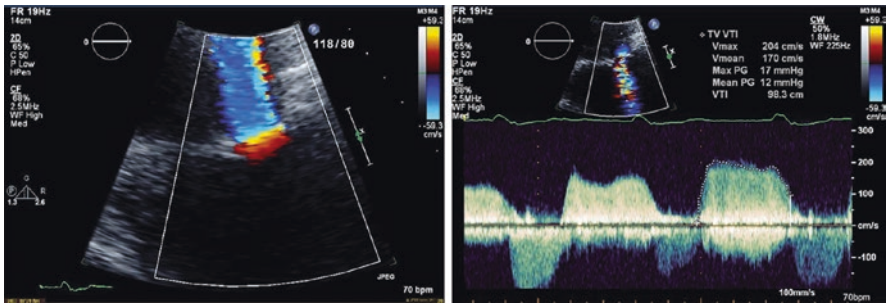

Fig. 5.8 Prosthetic tricuspid stenosis. Left: Zoomed apical four-chamber TTE view showing color flow acceleration across a 3-mm St. Jude tricuspid prosthetic valve during diastole, consistent with tricuspid stenosis (Video 5.5). Right: Transtricuspid prosthetic gradient shows a peak velocity of >2 m/s and a mean gradient of 12 mmHg, suggesting severe prosthetic stenosis

There is even less experience with the evaluation and assessment of tricuspid valves that were repaired percutaneously, as there are no FDA-approved devices at this time [46]. There are many devices that are currently in development, however. In the tricuspid edge-to-edge repair registry, the vena contracta, EROA, and regurgitant volume were calculated from multiple jets, and these methods will require validation [47].

Imaging for Tricuspid Valve Intervention

Emerging Therapies

Transcatheter therapies continue to evolve in light of the fact that a poor prognosis is associated with severe tricuspid regurgitation and also great morbidity and mortality associated with surgical intervention [48]. Percutaneous tricuspid valve procedures rely on accurate assessment of the tricuspid valve, both prior to and during the procedure, to determine correct placement. Imaging requirements vary based on the type of tricuspid regurgitation.

In order to determine which intervention is best, accurate assessment of tricuspid valve anatomy, mechanism of tricuspid regurgitation, and sizing of the annulus or vena cava is critical. Key features to take into account include the dimensions of the tricuspid annulus, the presence of a pacemaker lead across the valve and whether this is impacting valve function, and whether tricuspid valve leaflets prolapse or are fibrotic due to carcinoid or rheumatic disease [49].

Multimodality imaging is often needed in the face of complex pathology. Echocardiography is typically the first step to evaluate tricuspid valve anatomy and function, but assessment of the valve, annulus sizing, and right ventricular function is often complemented by the use of cardiac MRI (Chap. 6) and cardiac CT (Chap. 7).

Transcatheter Tricuspid Valve Interventions

Given the growing number of patients with severe tricuspid regurgitation who are at high surgical risk or inoperable, the emergence of transcatheter valve therapies may provide a feasible, durable, and safe solution [50]. At present, some key options available include heterotopic transcatheter valves within caval veins, tricuspid valve annuloplasty, the MitraClip device, and valve in valve/ring.

Heterotopic Transcatheter Valves

Tricuspid valve incompetence can lead to excess venous congestion so that implantation of balloon- or self-expandable transcatheter valves in the inferior vena cava and superior vena cava can decrease the backflow of blood. Therefore, patients with severe tricuspid regurgitation and systolic backflow reversal in the inferior vena cava may benefit from the placement of transcatheter valves. Distance between the cavoatrial junction and the first hepatic vein must be visualized as well as the caval vein dimensions and RV function prior to the procedure. This intervention was evaluated in the HOVER and TRICAVAL trials.

First, the severity of this tricuspid valve incompetence and RV function must be proven by TTE or CMR. Then, the dimensions of the caval veins and the distance from the inferior cavoatrial junction to the first hepatic vein must be determined by MDCT. If dimensions are smaller than desired, an obstruction could result upon tricuspid valve implantation. On the other hand, if the cavoatrial junction is too large, which may occur with right atrial dilation, there is a risk of device migration. Finally, if RV function is severely reduced, then further RA and RV remodeling, which can occur after device implantation due to elevated RA and RV pressures, may preclude symptomatic improvement [50].

Transcatheter Tricuspid Valve Annuloplasty Devices

Transcatheter tricuspid valve annuloplasty devices can be directly anchored into the tricuspid annulus (direct annuloplasty) or placed in the pericardial space along the atrioventricular groove (indirect annuloplasty). The PTVAS, SCOUT, and SCOUT II trials continue to evaluate both the safety and efficacy of direct annuloplasty approaches by way of the Trialign device. The PREVENT trial focuses on the safety and efficacy of an alternative direct annuloplasty device, the Tricinch device.

For direct annuloplasty, the first step is to determine the severity of functional tricuspid regurgitation by TTE or CMR. Then, MDCT is used to determine the course of the right coronary artery (RCA) along or, more rarely, across the atrioventricular groove. MDCT is also used in pre-procedure planning to obtain the distance between the RCA and the tricuspid annulus and to demarcate the atrioventricular groove. The course of the RCA and other epicardial coronary arteries is critical to prevent impingement during implantation of the device. If there is at least 2 mm between the RCA and tricuspid annulus, the anchors or pledgets of each device can safely avoid the RCA.

For indirect annuloplasty, it is important to locate the epicardial coronary arteries in relation to the atrioventricular groove to prevent impingement and ensure the coronary arteries do not cross the course of the transatrial intrapericardial tricuspid annuloplasty system. In addition, it must be confirmed that the lobe of the right atrial appendage is anterior since the pericardial space is accessed via the right atrial appendage [50].

In patients with secondary tricuspid regurgitation and only mild-moderate tricuspid annular dilation without significant tethering, an annuloplasty device remains a feasible option. These devices are currently being used in approximately 30% of patients. If there is more significant annular dilation and tethering, then annuloplasty could be used in combination with approaches such as the MitraClip device [51].

Edge-to-Edge Repair with the MitraClip Device

Since experimental models of functional tricuspid regurgitation demonstrated a significant reduction in EROA and regurgitant volume, which can concomitantly increase cardiac output, with clipping of septal and anterior leaflets, these techniques gained traction [52]. Tricuspid valve anatomy, localization of coaptation gap, and an assessment of which leaflets are most tethered are crucial to select the appropriate patients [50]. Planning prior to the procedure requires the determination of the largest vena contracta location and then the motion and length of the tricuspid leaflets.

Severity of tricuspid regurgitation must be assessed by TTE, TEE, or if needed CMR. Then to determine the largest EROA, TTE is crucial. To obtain further understanding of the coaptation gap and leaflet anatomy, 3D echo is critical due to high temporal and spatial resolution. If the coaptation gap between leaflets is too large or the tricuspid valve leaflets are excessively tethered, the procedure becomes more challenging. The MitraClip is best tolerated in those patients with primary tricuspid regurgitation due to tricuspid valve prolapse or pacemaker lead placement without severe tricuspid annular dilation. Secondary tricuspid regurgitation with only moderate tricuspid annular dilation or tethering may still benefit from the MitraClip. These devices currently represent the most common percutaneous transcatheter technology used, over 50% of the time. If the RV has remodeled significantly, and severe tricuspid annular dilation as well as tethering exists, then transcatheter valve replacement may be preferred [51].

Transcatheter Valve Replacement

If a patient has a failed tricuspid valve annuloplasty or a failed biological tricuspid prosthesis, there may be a benefit to a valve-in-ring or valve-in-valve procedure with the transcatheter Sapien valve or Melody valve.

Looking ahead prior to the procedure, first there must be an identification of the severity and mechanism of dysfunction by TTE. It is crucial to determine if there is paravalvular or valvular regurgitation. The dimensions of the ring or valve are also crucial—TTE, TEE, and MDCT can help accomplish these aims. If the sewing ring is incomplete, this leads to a shorter asymmetric landing zone for the deployment of transcatheter devices [50]. In addition, the size of the existing ring or prosthesis must be compatible with a transcatheter device. For those patients with primary TR due to rheumatic disease or lead placement with significant tricuspid annular

dilation, there is a role for transcatheter valve replacement. In patients with secondary tricuspid regurgitation but only moderate tricuspid annular dilation or with severe dilation but preserved or mildly reduced RV function, there can also be a role for transcatheter valve replacement. While various models of transcatheter valve replacement are developed, an adequately sized device can address significant annular dilation and also paravalvular leak found during planning stages [49].

Future Directions

In a recent study from the TriValve Registry of 312 high-risk patients with severe symptomatic tricuspid regurgitation, actuarial survival improved in those patients with successful device implantation. Furthermore, the main factor that was related to procedure failure was greater coaptation depth, a marker of valve tethering [53]. While this population was at increased risk and the registry enrolled patients with an eye toward the compassionate use of procedures, it helps provide insight into the potential for these procedures. The study also sheds light on the importance of patient selection; patients with late disease progression, with features such as RV remodeling and dysfunction, were less likely to experience procedural success. The field of transcatheter interventions for severe tricuspid regurgitation represents a new frontier, with questions such as scoring systems to predict eligibility, long-term durability, and anticoagulation, which remain under investigation. The novel devices explored here, alongside multimodality imaging techniques, will pave the way for innovative therapies to address a formidable disease process.

References

1. Hahn RT, Waxman AB, Denti P, Delhaas T. Anatomic relationship of the complex tricuspid valve, right ventricle, and pulmonary vasculature: a review. JAMA Cardiol. 2019;4(5):478–87.
2. Muraru D, Hahn RT, Soliman OI, Faletra FF, Basso C, Badano LP. 3-dimensional echocardiography in imaging the tricuspid valve. JACC Cardiovasc Imaging. 2019;12(3):500–15.
3. Khalique OK, Cavalcante JL, Shah D, Guta AC, Zhan Y, Piazza N, et al. Multimodality imaging of the tricuspid valve and right heart anatomy. JACC Cardiovasc Imaging. 2019;12(3):516–31.
4. Addetia K, Yamat M, Mediratta A, Medvedofsky D, Patel M, Ferrara P, et al. Comprehensive two-dimensional interrogation of the tricuspid valve using knowledge derived from three-dimensional echocardiography. J Am Soc Echocardiogr. 2016;29(1):74–82.
5. Hahn RT. State-of-the-art review of echocardiographic imaging in the evaluation and treatment of functional tricuspid regurgitation. Circ Cardiovas Imaging. 2016;9(12):e005332.
6. Taramasso M, Gavazzoni M, Pozzoli A, Dreyfus GD, Bolling SF, George I, et al. Tricuspid Regurgitation. JACC Cardiovasc Imaging. 2019;12(4):605–21.
7. Addetia K, Muraru D, Veronesi F, Jenei C, Cavalli G, Besser SA, et al. 3-dimensional echocardiographic analysis of the tricuspid annulus provides new insights into tricuspid valve geometry and dynamics. JACC: Cardiovasc Imaging. 2019;12:401–12.
8. Lancellotti P, Moura L, Pierard LA, Agricola E, Popescu BA, Tribouilloy C, Hagendorff A, Monin JL, Badano L, Zamorano JL. European Association of Echocardiography. European

Association of Echocardiography recommendations for the assessment of valvular regurgitation. Part 2: mitral and tricuspid regurgitation (native valve disease). Eur J Echocardiogr. 2010;11(4):307–32.
9. Nishimura RA, Otto CM, Bonow RO, Carabello BA, Erwin JP III, Guyton RA, O'Gara PT, Ruiz CE, Skubas NJ, Sorajja P, Sundt TM III, Thomas JD. 2014 AHA/ACC guideline for the management of patients with valvular heart disease: a report of the American College of Cardiology/American Heart Association Task Force on practice guidelines. Circulation. 2014;129:e521–643.
10. Hauck AJ, Freeman DP, Ackermann DM, Danielson GK, Edwards WD. Surgical pathology of the tricuspid valve: A study of 363 cases spanning 25 years. Mayo Clin Proc. 1988;63(9):851–63.
11. Nath J, Foster E, Heidenreich PA. Impact of tricuspid regurgitation on long-term survival. J Am Coll Cardiol. 2004;43(3):405–9.
12. Singh JP, Evans JC, Levy D, Larson MG, Freed LA, Fuller DL, et al. Prevalence and clinical determinants of mitral, tricuspid, and aortic regurgitation (the Framingham Heart Study). Am J Cardiol. 1999;83(6):897–902.
13. Mutlak D, Lessick J, Reisner SA, Aronson D, Dabbah S, Agmon Y. Echocardiography-based spectrum of severe tricuspid regurgitation: the frequency of apparently idiopathic tricuspid regurgitation. J Am Soc Echocardiogr. 2007;20(4):405–8.
14. He Y, Guo Y, Li Z, Chen J, Kontos MC, Paulsen WHJ, et al. Echocardiographic determination of the prevalence of primary myxomatous degeneration of the cardiac valves. J Am Soc Echocardiogr. 2011;24(4):399–404.
15. Come PC, Riley MF, Carl LV, Nakao S. Pulsed Doppler echocardiographic evaluation of valvular regurgitation in patients with mitral valve prolapse: comparison with normal subjects. J Am Coll Cardiol. 1986;8(6):1355–64.
16. van Son JAM, Miles CM, Starr A. Tricuspid valve prolapse associated with myxomatous degeneration. Ann Thorac Surg. 1995;59(5):1237.
17. Henein MY, O'Sullivan CA, Li W, Sheppard M, Ho Y, Pepper J, et al. Evidence for rheumatic valve disease in patients with severe tricuspid regurgitation long after mitral valve surgery: the role of 3D echo reconstruction. J Heart Valve Dis. 2003;12(5):566.
18. Bernal JM, Pontón A, Diaz B, Llorca J, García I, Sarralde A, et al. Surgery for rheumatic tricuspid valve disease: A 30-year experience. J Thorac Cardiovasc Surg. 2008;136(2):476–81.
19. Connolly HM, Pellikka PA. Carcinoid heart disease. Curr Cardiol Rep. 2006;8(2):96–101.
20. Bhattacharyya S, Davar J, Dreyfus G, Caplin ME. Carcinoid heart disease. Circulation. 2007;116(24):2860–5.
21. Attenhofer Jost CH, Connolly HM, Dearani JA, Edwards WD, Danielson GK. Ebstein's anomaly. Circulation. 2007;115(2):277.
22. Danielson GK, Driscoll DJ, Mair DD, Warnes CA, Oliver WC. Operative treatment of Ebstein's anomaly. J Thorac Cardiovasc Surg. 1992;104(5):1195–202.
23. Booker OJ, Nanda NC. Echocardiographic assessment of Ebstein's anomaly. Echocardiography. 2015;32(S2):S177–88.
24. Fanari Z, Hammami S, Hammami MB, Hammami S, Shuraih M. The effects of right ventricular apical pacing with transvenous pacemaker and implantable cardioverter defibrillator on mitral and tricuspid regurgitation. J Electrocardiol. 2015;48(5):791–7.
25. Addetia K, Harb SC, Hahn RT, Kapadia S, Lang RM. Cardiac implantable electronic device lead-induced tricuspid regurgitation. JACC Cardiovasc Imaging. 2019;12(4):622–36.
26. Mediratta A, Addetia K, Yamat M, Moss JD, Nayak HM, Burke MC, et al. 3D echocardiographic location of implantable device leads and mechanism of associated tricuspid regurgitation. JACC Cardiovasc Imaging. 2014;7(4):337–47.
27. Seo Y, Ishizu T, Nakajima H, Sekiguchi Y, Watanabe S, Aonuma K. Clinical utility of 3-dimensional echocardiography in the evaluation of tricuspid regurgitation caused by pacemaker leads. Circ J. 2008;72(9):1465–70.

28. Vaturi M, Kusniec J, Shapira Y, Nevzorov R, Yedidya I, Weisenberg D, et al. Right ventricular pacing increases tricuspid regurgitation grade regardless of the mechanical interference to the valve by the electrode. Eur J Echocardiogr. 2010;11(6):550–3.
29. Prihadi EA, Delgado V, Leon MB, Enriquez-Sarano M, Topilsky Y, Bax JJ. Morphologic types of tricuspid regurgitation: characteristics and prognostic implications. JACC Cardiovasc Imaging. 2019;12(3):491–9.
30. Bartko PE, Arfsten H, Frey MK, Heitzinger G, Pavo N, Cho A, et al. Natural history of functional tricuspid regurgitation: implications of quantitative Doppler assessment. JACC Cardiovasc Imaging. 2019;12(3):389–97.
31. Bustamante-Labarta M, Perrone S, de la Fuente RL, Stutzbach P, de la Hoz RP, Torino A, et al. Right atrial size and tricuspid regurgitation severity predict mortality or transplantation in primary pulmonary hypertension. J Am Soc Echocardiogr. 2002;15(10):1160–4.
32. Utsunomiya H, Itabashi Y, Mihara H, Berdejo J, Kobayashi S, Siegel RJ, et al. Functional tricuspid regurgitation caused by chronic atrial fibrillation: a real-time 3-dimensional transesophageal echocardiography study. Circ Cardiovasc Imaging. 2017;10(1):e004897.
33. Topilsky Y, Nkomo VT, Vatury O, Michelena HI, Letourneau T, Suri RM, et al. Clinical outcome of isolated tricuspid regurgitation. J Am Coll Cardiol Img. 2014;7(12):1185–94.
34. Fender EA, Zack CJ, Nishimura RA. Isolated tricuspid regurgitation: outcomes and therapeutic interventions. Heart. 2018;104(10):798–806.
35. Hahn RT, Delhaas T, Denti P, Waxman AB. The tricuspid valve relationship with the right ventricle and pulmonary vasculature. J Am Coll Cardiol Img. 2019;12(3):559–71.
36. Zoghbi WA, Adams D, Bonow RO, Enriquez-Sarano M, Foster E, Grayburn PA, et al. Recommendations for noninvasive evaluation of native valvular regurgitation. J Am Soc Echocardiogr. 2017;30(4):303–71.
37. Hahn RT, Thomas JD, Khalique OK, Cavalcante JL, Praz F, Zoghbi WA. Imaging assessment of tricuspid regurgitation severity. J Am Coll Cardiol Img. 2019;12(3):469–90.
38. Thomas JD, Liu CM, Flachskampf FA, O'Shea JP, Davidoff R, Weyman AE. Quantification of jet flow by momentum analysis. An in vitro color Doppler flow study. Circulation. 1990;81(1):247.
39. Song JM, Jang MK, Choi YS, Kim YJ, Min SY, Kim DH, et al. The vena contracta in functional tricuspid regurgitation: a real-time three-dimensional color Doppler echocardiography study. J Am Soc Echocardiogr. 2011;24(6):663–70.
40. Hahn RT, Zamorano JL. The need for a new tricuspid regurgitation grading scheme. Eur Heart J Cardiovasc Imaging. 2017;18(12):1342–3.
41. Waller BF. Pathology of TS and TR (Part III). Clin Cardiol. 1995;18(4):225–30. https://pubmed.ncbi.nlm.nih.gov/7788951/.
42. Baumgartner H, Hung J, Bermejo J, Chambers JB, Evangelista A, Griffin BP, et al. Echocardiographic assessment of valve stenosis: EAE/ASE recommendations for clinical practice. Eur J Echocardiogr. 2009;10(1):1–25.
43. Zoghbi WA, Chambers JB, Dumesnil JG, Foster E, Gottdiener JS, Grayburn PA, et al. Recommendations for evaluation of prosthetic valves with echocardiography and Doppler ultrasound. A report from the American Society of Echocardiography's Guidelines and Standards Committee and the Task Force on prosthetic valves, developed in conjunction. J Am Soc Echocardiogr. 2009;22(9):975–1014.
44. Blauwet LA, Danielson GK, Burkhart HM, Dearani JA, Malouf JF, Connolly HM, et al. Comprehensive echocardiographic assessment of the hemodynamic parameters of 285 tricuspid valve bioprostheses early after implantation. J Am Soc Echocardiogr. 2010;23(10):1045–59.e2.
45. Blauwet LA, Burkhart HM, Dearani JA, Malouf JF, Connolly HM, Hodge DO, et al. Comprehensive echocardiographic assessment of mechanical tricuspid valve prostheses based on early post-implantation echocardiographic studies. J Am Soc Echocardiogr. 2011;24(4):414–24.
46. Zoghbi WA, Asch FM, Bruce C, Gillam LD, Grayburn PA, Hahn RT, et al. Guidelines for the evaluation of valvular regurgitation after percutaneous valve repair or replacement: a report

from the American Society of Echocardiography Developed in Collaboration with the Society for Cardiovascular Angiography and Interventions, Japanese Society of Echocardiography, and Society for Cardiovascular Magnetic Resonance. J Am Soc Echocardiogr. 2019;32(4):431–75.
47. Nickenig G, Kowalski M, Hausleiter J, Braun D, Schofer J, Yzeiraj E, et al. Transcatheter treatment of severe tricuspid regurgitation with the edge-to-edge MitraClip technique. Circulation. 2017;135(19):1802–14.
48. Pozzoli A, Elisabetta L, Vicentini L, Alfieri O, De Bonis M. Surgical indication for functional tricuspid regurgitation at initial operation: judging from long term outcomes. Gen Thorac Cardiovasc Surg. 2016;64(9):509–16.
49. Demir OM, Regazzoli D, Mangieri A, Ancona MB, Mitomo S, Weisz G, et al. Transcatheter tricuspid valve replacement: principles and design. Front Cardiovasc Med. 2018;5:129.
50. Prihadi EA, Delgado V, Hahn RT, Leipsic J, Min JK, Bax JJ. Imaging needs in novel transcatheter tricuspid valve interventions. JACC Cardiovasc Imaging. 2018;11(5):736–54.
51. Asmarats L, Puri R, Latib A, Navia JL, Rodés-Cabau J. Transcatheter tricuspid valve interventions: landscape, challenges, and future directions. J Am Coll Cardiol. 2018;71(25):2935–56.
52. Vismara R, Gelpi G, Prabhu S, Romitelli P, Troxler LG, Mangini A, Romagnoni C, Contino M, Van Hoven DT, Lucherini F, Jaworek M, Redaelli A, Fiore GB, Antona C. Transcatheter edge-to-edge treatment of functional tricuspid regurgitation in an ex vivo pulsatile heart model. J Am Coll Cardiol. 2016;68(10):1024–33.
53. Taramasso M, Alessandrini H, Latib A, Asami M, Attinger-Toller A, Biasco L, et al. Outcomes after current transcatheter tricuspid valve intervention. JACC: Cardiovasc Interv. 2019;12(2):155–65.